

Special  
Collection

# Discovery of a Lead Brain-Penetrating Gonadotropin-Releasing Hormone Receptor Antagonist with Saturable Binding in Brain

Roberto B. W. Bekker,<sup>[a]</sup> Richard Fjellaksel,<sup>[b, c, d]</sup> Trine Hjørnevik,<sup>[e]</sup> Syed Nuruddin,<sup>[f]</sup> Waqas Rafique,<sup>[a]</sup> Jørn H. Hansen,<sup>[d]</sup> Rune Sundset,<sup>[b, c]</sup> Ira H. Haraldsen,<sup>[g]</sup> and Patrick J. Riss<sup>\*[a, f, g]</sup>

We report the synthesis, radiosynthesis and biological characterisation of two gonadotropin-releasing hormone receptor (GnRH-R) antagonists with nanomolar binding affinity. A small library of GnRH-R antagonists was synthesised in 20–67% overall yield with the aim of identifying a high-affinity antagonist capable of crossing the blood–brain barrier. Binding affinity to rat GnRH-R was determined by autoradiography in competitive-binding studies against [<sup>125</sup>I]buserelin, and inhibition constants were calculated by using the Cheng–Prusoff equation. The radioligands were obtained in 46–79% radiochemical yield and >95% purity and with a molar activity of 19–38 MBq/nmol by direct nucleophilic radiofluorination. Positron emission tomography imaging in rat under baseline

conditions in comparison to pretreatment with a receptor-saturating dose of GnRH antagonist revealed saturable uptake (0.1 %ID/mL) into the brain.

Our attention has been drawn towards the gonadotropin releasing hormone receptor (GnRH-R) because of its role in hormone related behaviour and in the pathophysiology of several diseases. Gonadotropin releasing hormone is a decapeptide hormone (pyroGlu-His-Trp-Ser-Tyr-Gly-Leu-Arg-Pro-Gly-NH<sub>2</sub>) and a key neurotransmitter in the hypothalamus-pituitary-gonadal axis. Apart from the classical role in reproduction, GnRH plays a role in cell proliferation,<sup>[1,2]</sup> tumour progression,<sup>[3–5]</sup> metastasis<sup>[4]</sup> and angiogenesis,<sup>[5]</sup> and has been linked to neurodegenerative cascades, for example, in dementia through nonclassical mechanisms.<sup>[6–8]</sup> In circulation, the peptide acts as an endocrine signalling hormone that mediates the release of follicle stimulating hormone and luteinising hormone by GnRH-R activation in the pituitary gland and other regions.<sup>[2,5–8]</sup> As such, hormonal signalling cascades following GnRH-R activation might catalyse the multiple actions of GnRH and mediate hormone signalling in the central nervous system (CNS). The GnRH-R is widely expressed in CNS; highest levels are found in the olfactory bulb, hypothalamus, and hippocampus.<sup>[5,7–9]</sup> Furthermore, GnRH-R plays an established role in clinical care, for example, in the treatment of hormone-responsive cancers, reproductive disorders and for behavioural modification of sexual offenders through these mechanisms. Recent observations also demonstrate crosstalk between GnRH-R and growth factor receptors.<sup>[1–6]</sup>

Few publications have investigated GnRH-R antagonists for PET. However, the role GnRH plays in pathophysiology of diseases emphasises the potential of GnRH-R PET imaging.

In this study our main goal was to develop a PET imaging probe for GnRH-R in brain.<sup>[16–18]</sup> In more detail, we were interested in the development of a moderate-strength GnRH-R antagonist to target brain imaging of GnRH-R as means to detect and characterise brain cancer, both primary tumours and metastases, as well as to elucidate CNS mechanisms of behaviour, brain damage and cognition involving GnRH-R.<sup>[9–11]</sup>

In our reasoning, a reversibly binding antagonist of GnRH-R would be particularly interesting because of its lack of receptor stimulatory side effects and superior passive tissue permeability to peptide agonists.<sup>[12]</sup>

[a] R. B. W. Bekker, Dr. W. Rafique, Prof. P. J. Riss  
Department of Chemistry, University of Oslo  
Sem Sælands vei, 260371 Oslo (Norway)  
E-mail: Patrick.Riss@kjemi.uio.no

[b] Dr. R. Fjellaksel, Prof. R. Sundset  
Department of Clinical Medicine  
UiT The Arctic University of Norway  
Hansine Hansens veg 18  
9019 Tromsø (Norway)

[c] Dr. R. Fjellaksel, Prof. R. Sundset  
PET Imaging Center  
University Hospital of North Norway  
Sykehusvegen 38, 9019 Tromsø (Norway)

[d] Dr. R. Fjellaksel, Prof. J. H. Hansen  
Department of Chemistry  
UiT – The Arctic University of Norway  
Hansine Hansens veg 18  
9019 Tromsø (Norway)

[e] Dr. T. Hjørnevik  
Department of Diagnostic Physics  
Oslo University Hospital  
Sognsvannsveien 20, 0372 Oslo (Norway)

[f] Dr. S. Nuruddin, Prof. P. J. Riss  
Norwegian Medical Cyclotron AS, Rikshospitalet  
Sognsvannsveien 20, Oslo, (Norway)

[g] Dr. I. H. Haraldsen, Prof. P. J. Riss  
Clinical Neurosciences  
Oslo University Hospital-Ullevål  
Kirkeveien 166, post code? Oslo (Norway)

Supporting information for this article is available on the WWW under <https://doi.org/10.1002/cmdc.202000256>

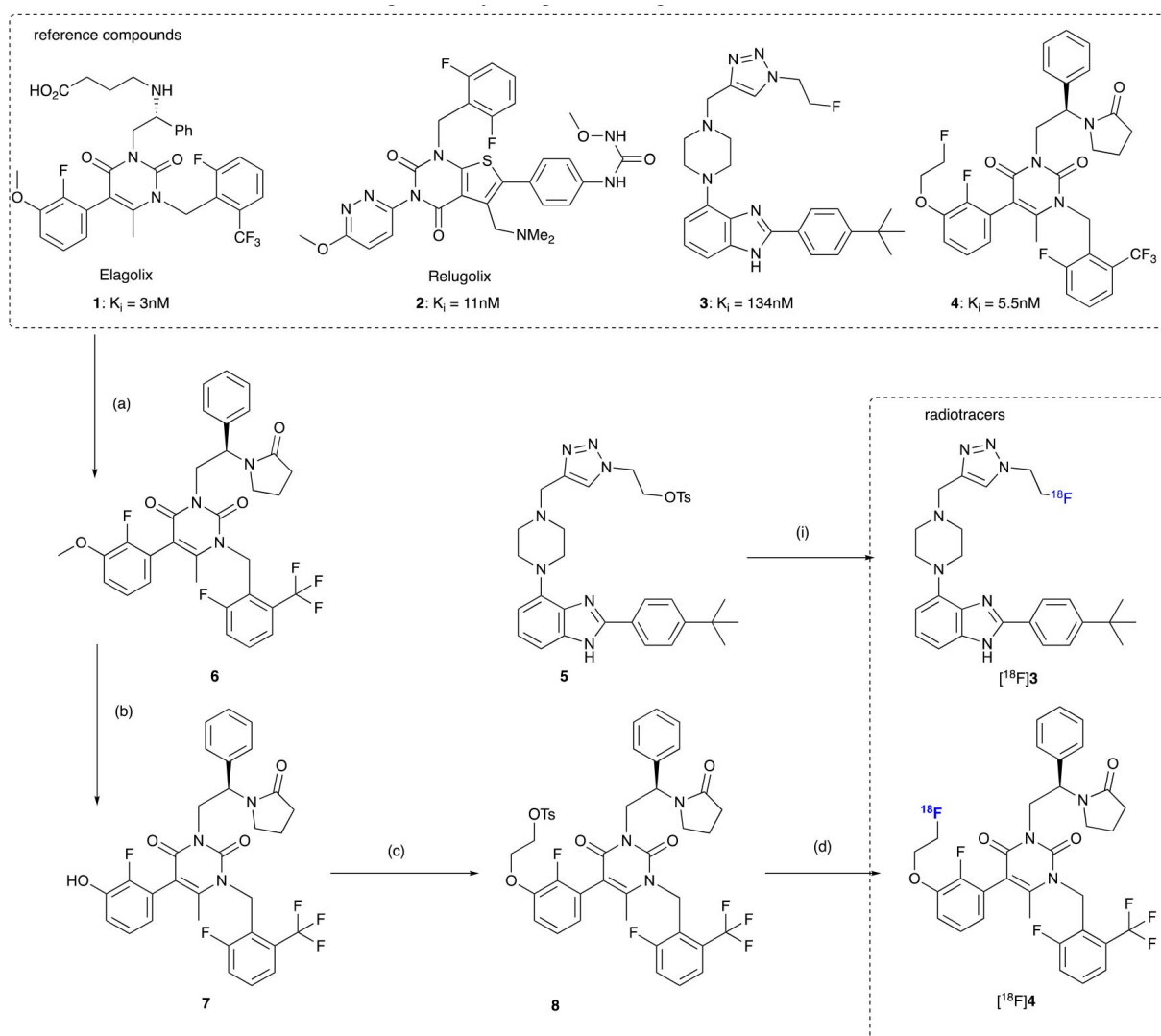
This article belongs to the Special Collection “Nordic Medicinal Chemistry 2019–2020”

© 2020 The Authors. Published by Wiley-VCH GmbH.  
This is an open access article under the terms of the Creative Commons Attribution Non-Commercial NoDerivs License, which permits use and distribution in any medium, provided the original work is properly cited, the use is non-commercial and no modifications or adaptations are made.

Several classes of small-molecular antagonist have been investigated for imaging GnRH-R, and tested for positron emission tomography (PET) imaging in the brain, however, without success.<sup>[13–14]</sup> The authors point out several reasons for failure such as affinity, molecular size and association kinetics. We have pursued a library of GnRH-R antagonists that addresses the moderate to high-affinity range allowing competition of the ligand in circulation with endogenous GnRH at GnRH-R binding sites. While the use of moderate affinity antagonists may permit assessment of the receptor availability, a measure reflecting both ligand concentration and the concentration of the receptor in tissues, high-affinity ligands may be required to image low concentration targets. Elagolix (1) and relugolix (2) are potent small-molecule GnRH antagonists from a novel class drugs unrelated to the earlier peptide-based ligands (Scheme 1). Given the pharmacokinetic profiles of these approved drugs, we were certain that 1 and 2 would not suffer from metabolic instability. At the same time, the high

lipophilicity ( $\log D_{7.4}$ ) of 4 and 4.6, respectively, held promise of decent brain uptake. Based on these considerations and previous work wherein structure–activity relationships, affinity and off target binding were assessed, we selected benzimidazol-derivative 3 and elagolix analogue 4, for further study.<sup>[12,15–18]</sup> The primary objective in developing GnRH-R radiotracers for brain imaging is achieving brain uptake and saturable binding in brain, which has been elusive so far.

Reference 3 and the corresponding labelling precursor 5 were obtained by copper-mediated azide-alkyne cycloaddition as described previously; however, 1.05 equiv. Cu was required to achieve useful conversion of the starting material.<sup>[13]</sup> Compound 6 was prepared by cyclisation of elagolix using bis 2-methylprop-2-yl pyrocarbonate in MeCN in a yield of 92% (a). Demethylation was achieved using boron tribromide in dichloromethane furnish compound 7 in 64% yield (b). Compound 7 was converted into the reference compound 4 ((R)-5-(2-fluoro-3-(2-fluoroeth-1-oxy)phenyl)-1-(2-fluoro-6-



**Scheme 1.** Competitive binding affinities ( $K_i$ ) for compounds 1–4 and synthetic route for radiolabelling compounds [ $^{18}\text{F}$ ]3 and [ $^{18}\text{F}$ ]4: a) BOC<sub>2</sub>O, DMAP, MeCN, 92%; b) BBr<sub>3</sub>, CH<sub>2</sub>Cl<sub>2</sub>, 64%; c) Cs<sub>2</sub>CO<sub>3</sub>, ethylene ditosylate, MeCN, 64%; d) crypt-222, K<sub>2</sub>CO<sub>3</sub>, MeCN, 79%; i) crypt-222, K<sub>2</sub>CO<sub>3</sub>, MeCN, 46%.

(trifluoromethyl)benzyl)-6-methyl-3-(2-(2-oxopyrrolidin-1-yl)-2-phenylethyl)pyrimidine-2,4(1*H*,3*H*)-dione) by using 2-fluoro ethyl 4-methylbenzenesulfonate dissolved in anhydrous MeCN with cesium carbonate as base in up to 40% yield (c). The labelling precursor (*R*)-2-(2-fluoro-3-(1-(2-fluoro-6-(trifluoromethyl)benzyl)-6-methyl-2,4-dioxo-3-(2-(2-oxopyrrolidin-1-yl)-2-phenylethyl)-1,2,3,4-tetrahydropyrimidin-5-yl)-phenoxy)ethyl 4-methylbenzene sulfonate (**8**) was obtained in a yield of 64% by treating **7** with an excess of ethylene ditosylate in MeCN (d). The purity of each compound was determined by reversed-phase HPLC prior to testing of the compounds' binding affinity.

Competition binding experiments were conducted on flash-frozen transversal brain sections (rat, 20  $\mu$ m thickness), thaw mounted on microscope slides. Following optimisation of times, temperatures and radioligand concentration, experiments were conducted with [<sup>125</sup>I]buserelin ( $A_M=81.4$  MBq/nmol) at 22 °C. Sections were incubated in assay buffer for 90 minutes in presence of [<sup>125</sup>I]buserelin (0.6 nM) using eleven different concentrations of test compounds in four separate experiments. Nonspecific binding was determined using buserelin.<sup>[19,20]</sup> A BAS MS imaging screen was exposed to the activity-loaded sections for 2 weeks. The screen was then analysed with a Duerr phosphor imager and [<sup>125</sup>I]Buserelin radioactivity in hippocampus was determined to obtain  $IC_{50}$  values using ray-test AIDA image analysis software.  $IC_{50}$  values were obtained from nonlinear curve fitting of the values obtained in individual experiments and  $K_i$  values were calculated (Table 1).<sup>[21]</sup>

In order to test the brain uptake of the lead compounds, radiosynthesis conditions for production and formulation of [<sup>18</sup>F]**3** and [<sup>18</sup>F]**4** were developed. Here, DMSO proved useful for labelling, but spoiled the use of simple HPLC conditions. DMF gave low yield unless heated to high temperature at which point the molar activity of the product became unacceptably low. MeCN was a charm to work with for purification, however, it had to be heated beyond its boiling point in tightly capped vials to achieve high conversion of [<sup>18</sup>F]fluoride ion within 10 minutes. After some optimisation, both compounds were produced using 3 mg of precursors **5** and **8**, respectively, for direct, aliphatic nucleophilic radiofluorination in acetonitrile at 90 °C for 10 minutes.<sup>[18]</sup>

Under these conditions, [<sup>18</sup>F]**3** was formed in a radiochemical yield of  $46 \pm 2\%$  and [<sup>18</sup>F]**4** was formed in a radiochemical yield of  $79 \pm 1\%$ . At the end of the labelling reaction, the reaction mixtures were diluted with MeCN/H<sub>2</sub>O (1:1, 0.7 mL) and injected into a preparative HPLC system to purify the labelled product. Radiotracer [<sup>18</sup>F]**3** was purified on a Merck Chromolith RP18 column (150  $\times$  10 mm) using MeOH-

Ammonium formate (0.1 M, pH 7); 1:1 as mobile phase at a flow rate of 8.5 mL/min. The HPLC fraction containing the product was collected 7–9 min after the injection. The product fraction was diluted and [<sup>18</sup>F]**3** was extracted using a waters SepPak plus C<sub>18</sub> cartridge pre-rinsed with EtOH and water. The cartridge was washed with H<sub>2</sub>O (10 mL) afterwards and the retained product was eluted into a clean glass vial with endotoxin free physiological saline (0.9% NaCl) using EtOH (< 10%). The tracer was obtained in a nondecay corrected activity yield of 11% (380 MBq) with a molar activity of 18.5 MBq/nmol at delivery to the scanner. Candidate [<sup>18</sup>F]**4** was purified on a Supelco HS-F5 column (250  $\times$  10 mm) with MeCN/water (55:45) as mobile phase at a flow rate of 5 mL/min.

The HPLC fraction containing the product was collected ( $t_R=11-12$  min) in a round bottomed flask, diluted with water (50 mL) and extracted via solid phase extraction (Phenomenex Strata X C<sub>18</sub>) pre-rinsed with EtOH and water. The cartridge was washed with H<sub>2</sub>O (10 mL) afterwards and the retained product was eluted into a clean glass vial with endotoxin free physiological saline (0.9% NaCl) using EtOH (<10%) in an activity yield of 52% (uncorrected; 1.38 GBq) and a molar activity of 38 MBq/nmol. The QC samples were analysed while the radiotracers were shipped to the imaging facility. Both radiotracers had a radiochemical purity >95% at the time of injection.<sup>[22]</sup>

Animal experiments were conducted in accordance with national Norwegian regulations on the use of laboratory animals in research (FOR-2015-06-18-761), decision regarding the use of animals in procedures - FOTS ID 12701, establishment number 016: UiO-Institutt for medisinske basalfag (Domus Medica). Processed by the Norwegian Food Safety Authority (NFSA), 28.06.2017.

Imaging was conducted in female Sprague Dawley rats (13  $\pm$  1 months of age, 379  $\pm$  23 g,  $n=4$ ). The animals were anaesthetised during the procedure, body temperature was monitored using a rectal probe and maintained at 37 °C. Anaesthesia was initialised with 5% isoflurane in air which was reduced to 2% isoflurane for maintenance. The tail vein was catheterised, and a saline plug was used to ensure that the catheter was placed correctly and probes to record the respiration and heart rate were connected accordingly. The tracer (21  $\pm$  4 MBq, in 0.5  $\pm$  0.1 mL) was injected through the catheter as slow bolus injection, For baseline scans, rats were imaged at a dose of 2 nmol/kg, for blocking studies, animals were pretreated with relugolix (3.5  $\mu$ mol/kg) prior to injection of 4 nmol/kg of the radiotracer. Each animal was scanned for 60 minutes. More information about the scanning protocol can be found in the supporting information. Animals for harvesting were not scanned and euthanised after 45 minutes. After re-test of [<sup>18</sup>F]**4**, blood samples were taken from two further animals ( $ID=38 \pm 3$  MBq) for 45 minutes and worked up for determination of radioactive metabolites. In brief, a blood sample (100  $\mu$ L) was centrifuged at 5000 rpm (Eppendorf MiniSpin plus centrifuge) for 5 minutes. 50  $\mu$ L of supernatant was taken and transferred into a secondary Eppendorf vial containing methanol. The Eppendorf vial was centrifuged for further 5 minutes. The supernatant was injected directly into the analytic HPLC

**Table 1.** Binding affinity to rat GnRH receptors as determined from competitive binding studies against [<sup>125</sup>I]buserelin.

Compound	$IC_{50}$ [nM]	$K_i$ [nM]
1	4.85 $\pm$ 0.29	3.02 $\pm$ 0.29
2	17.5 $\pm$ 0.4	10.9 $\pm$ 0.4
3	215 $\pm$ 1	134 $\pm$ 1
4	8.7 $\pm$ 0.39	5.49 $\pm$ 0.39

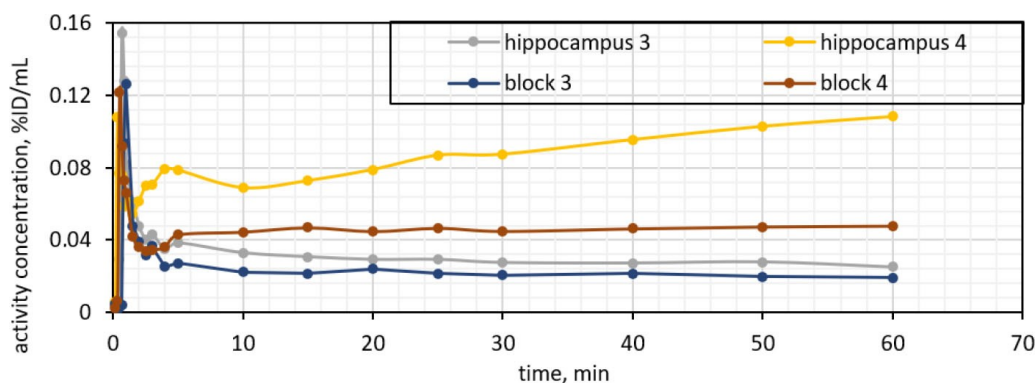


**Figure 1.** On the left side: Time activity curves for compounds  $[^{18}\text{F}]\mathbf{3}$  and  $[^{18}\text{F}]\mathbf{4}$  in the hippocampus (HIP) brain region of interest for representative animal brains coregistered to an atlas with regions of interest. On the right side: MRI atlas with ROI delineated on HIP and PET/MR fusion image of similar brain slice with  $[^{18}\text{F}]\mathbf{4}$ .

and spotted on TLC to separate blood metabolites from intact radiotracer. Brain was harvested right after euthanising at 45 min p.i. and homogenised by grinding in methanol in a glass tissue homogeniser for 5 minutes. After standing for few minutes, 500  $\mu\text{L}$  from the top layer was transferred into an Eppendorf vial and centrifuged for 5 minutes. This supernatant was injected into analytical HPLC and spotted on TLC to check for brain metabolites. HPLC was evaluated by collection of the eluate in fractions and counting in a NaI well counter. No intact  $[^{18}\text{F}]\mathbf{3}$  was found in the plasma supernatant; however, all residual activity in blood was located in the precipitated protein pellet which could be explained by near quantitative protein binding of  $[^{18}\text{F}]\mathbf{3}$  or by its inherently low solubility of 2  $\mu\text{g}/\text{mL}$  at pH 7.4. Unfortunately, activity in brain 60 min p.i. did not suffice for detection or identification of the radiometabolites of compound  $[^{18}\text{F}]\mathbf{3}$  as the residual count rate was below the limit of quantification. For compound  $[^{18}\text{F}]\mathbf{4}$ , more than 95% of the residual activity in blood were intact radiotracer, only  $[^{18}\text{F}]\mathbf{4}$  was detected in brain with a corresponding distribution volume of 1.05.<sup>[22]</sup>

Other studies of GnRH-R antagonist have shown low brain penetration.<sup>[14]</sup> However, in our study both tracers enter the brain in a tenfold higher concentration as shown in Figure 1. Whereas  $[^{18}\text{F}]\mathbf{3}$  washes out quickly and shows negligible effect of blocking,  $[^{18}\text{F}]\mathbf{4}$  shows a steady accumulation in brain, albeit at a slow rate after an initial peak. In order to confirm displaceable binding in brain, animals ( $n=2$ ) were pretreated with relugolix to reduce availability of the GnRH-R. Relugolix was given as a single dose 10 minutes prior to administration of the radiotracer and animals were scanned for 60 minutes. Although the receptor-saturating dose only marginally reduced  $[^{18}\text{F}]\mathbf{3}$  binding in GnRH rich regions, uptake increased in regions with low GnRH expression at higher concentrations (up to 10% in thalamus), possibly due to saturation of peripheral sites or active transport of the tracer out of the brain, a clear effect of the pretreatment was observed for  $[^{18}\text{F}]\mathbf{4}$  ( $[^{18}\text{F}]\mathbf{3}$ : -28%;  $[^{18}\text{F}]\mathbf{4}$ : -80% of specific binding); this is the first time such an effect has been observed for GnRH radiotracers in the brain. Given that the radiotracer was employed at a rather mediocre molar

activity, the pronounced mass dependency of the binding might have resulted in a reduction of the specific even under the baseline conditions. One may surmise that a somewhat better performance could be expected when using a radiotracer with a higher molar activity than  $[^{18}\text{F}]\mathbf{4}$  in the present study. Although the indication of some blockable uptake is a major success, we suspect that the high molar mass of  $[^{18}\text{F}]\mathbf{4}$  is a key factor leading to the slow kinetics with increasing uptake over 60 minutes p.i.<sup>[23]</sup> On the other hand, the low nanomolar affinity of  $\mathbf{3}$  does seem to lead to saturable, detectable binding, it does not seem high enough yet for successful imaging of GnRH containing brain regions.

In conclusion, we have developed and tested two new radiotracer candidates for PET imaging of GnRH-R in brain. One of the candidates, compound  $[^{18}\text{F}]\mathbf{4}$ , shows for the first time brain penetration and displaceable accumulation at GnRH-R specific sites in the brain. Additionally,  $[^{18}\text{F}]\mathbf{4}$  is a promising lead structure for further developmental work targeting higher binding affinity paired with a somewhat lower molar mass.

## Conflict of Interest

The authors declare no conflict of interest.

**Keywords:** elagolix · fluorine-18 · GnRH-R · GnRH · PET

- [1] J. B. Engel, A. V. Schally, *Nat. Clin. Pract. Endocrinol. Metab.* **2007**, *3*, 157–167.
- [2] H. Van Poppel, S. Nilsson, *Urology* **2008**, *71*, 1001–1006.
- [3] R. L. Gustofson, J. H. Segars, F. W. Larsen, *Hum. Reprod.* **2006**, *21*, 2830–2837.
- [4] S. Meethal, M. Smith, R. Bowen, C. Atwood, *Endocrine* **2005**, *3*, 317–325.
- [5] A. Aguilar-Rojas, M. Huerta-Reyes, *Oncol. Rep.* **2009**, *5*, 981–990.
- [6] L. W. Cheung, A. S. Wong, *FEBS J.* **2008**, *22*, 5479–5496.
- [7] D. C. Skinner, A. J. Albertson, A. Navaratil, A. Smith, M. Mignot, H. Talbott, N. Scanlan-Blake, *J. Neuroendocrinol.* **2009**, *4*, 282–292.
- [8] J. L. Quintranar, E. Salinas, *Neurochem. Res.* **2008**, *33*, 1051–1056.
- [9] G. Zhang, J. Li, S. Purkayastha, Y. Tang, H. Zhang, Y. Yin, B. Li, G. Liu, D. Cai, *Nature* **2013**, *497*, 211–216.
- [10] P. Brilken, A. Hill, W. Berner, *J. Clin. Psychiatry* **2003**, *8*, 890–897.

- [11] C. Eisenegger, M. Naef, R. Snozzi, M. Heinrichs, E. Fehr, *Nature* **2010**, *463*, 356–359.
- [12] K. Virdee, P. Cumming, D. Carpioli, B. Jupp, A. Rominger, F. I. Aigbirhio, T. D. Fryer, P. J. Riss, J. W. Dalley, *Neuroscience and Biobehavioural Reviews* **2012**, *36*, 1188–1216.
- [13] D. E. Olberg, N. Bauer, K. W. Andressen, T. Hjørnevik, P. Cummings, F. O. Levy, J. Klaveness, I. Haraldsen, J. L. Sutcliffe, *Nucl. Med. Biol.* **2016**, *43*, 478–489.
- [14] D. E. Olberg, K. W. Andressen, F. O. Levy, J. Klaveness, I. Haraldsen, J. L. Sutcliffe, *Bioorg. Med. Chem. Lett.* **2014**, *24*, 1846–1850.
- [15] C. Chen, D. Wu, Z. Guo, Q. Xie, G. J. Reinhart, A. Madan, J. Wen, T. Chen, C. Q. Huang, M. Chen, Y. Chen, F. C. Tucci, M. Rowbottom, J. Pontillo, Y. Zhu, W. Wade, J. Saunders, H. Bozigian, R. S. Struthers, *J. Med. Chem.* **2008**, *51*, 7478–7485.
- [16] R. Fjellaksel, M. Boomgaren, R. Sundset, I. H. Haraldsen, J. H. Hansen, P. J. Riss, *MedChemComm* **2017**, *8*, 1965–1969.
- [17] F. L. Tukun, D. E. Olberg, P. J. Riss, I. H. Haraldsen, A. Kaass, J. Klaveness, *Molecules* **2017**, *12*, 2188.
- [18] R. Fjellaksel, A. Moldes-Anaya, T. Vasskog, A. Oteiza, M. Martin-Armas, O. K. Hjelstuen, J. H. Hansen, P. J. Riss, R. Sundset, *J. Labelled Compd. Radiopharm.* **2019**, *63*, 72–84.
- [19] T. A. Bramley, C. A. McPhie, G. S. Menzies, *Placenta* **1992**, *13*, 555–581.
- [20] G. S. Menzies, T. A. Bramley, *Placenta* **1992**, *13*, 583–595.
- [21] Y. Cheng, W. H. Prusoff, *Biochem. Pharmacol.* **1973**, *23*, 3099–3108.
- [22] P. J. Riss, Y. T. Hong, J. Marton, D. Caprioli, D. J. Williamson, V. Ferrari, N. Saigal, B. L. Roth, G. Henriksen, T. D. Fryer, J. W. Dalley, F. I. Aigbirhio, *J. Nuclear Med.* **2013**, *54*, 299–305.
- [23] M. Kuna, F. Mahdi, A. R. Chade, G. L. Bidwell III, *Sci. Rep.* **2018**, *8*, 7923.

---

Manuscript received: April 21, 2020  
Revised manuscript received: July 12, 2020  
Accepted manuscript online: July 16, 2020  
Version of record online: August 10, 2020